Quantum dimer model with $\mathbb{Z}_2$ liquid ground state: Interpolation between cylinder and disk topologies and toy model for a topological quantum bit

Grégoire Misguich and Vincent Pasquier
Service de Physique Théorique, CEA-Saclay, 91191 Gif-sur-Yvette Cédex, France

Frédéric Mila
Institut de Théorie des Phénomènes Physiques, École Polytechnique Fédérale de Lausanne BSP, CH-1015 Lausanne, Switzerland

Claire Lhuillier
Laboratoire de Physique Théorique des Liquides, Université Pierre et Marie Curie and UMR 7600 of CNRS, Case 121, 4 Place Jussieu, 75252 Paris Cédex, France

(Received 27 October 2004; published 27 May 2005)

We consider a quantum dimer model on the kagome lattice, which was introduced recently [Phys. Rev. Lett. **89**, 137202 (2002)]. It realizes a $\mathbb{Z}_2$ liquid phase and its spectrum was obtained exactly. It displays a topological degeneracy when the lattice has a nontrivial geometry (cylinder, torus, etc). We discuss and solve two extensions of the model where perturbations along lines are introduced: first a potential-energy term repelling (or attracting) the dimers along a line and second, a perturbation allowing to create, move, or destroy monomers. For each of these perturbations we show that there exists a critical value above which, in the thermodynamic limit, the degeneracy of the ground state is lifted from 2 (on a cylinder) to 1. In both cases the exact value of the gap between the first two levels is obtained by a mapping to an Ising chain in a transverse field. This model provides an example of a solvable Hamiltonian for a topological quantum bit where the two perturbations act as diagonal and transverse operators in the two-dimensional subspace. We discuss how crossing the transitions may be used in the manipulation of the quantum bit to simultaneously optimize the frequency of operation and the losses due to decoherence.

DOI: 10.1103/PhysRevB.71.184424 PACS number(s): 75.10.Jm

I. INTRODUCTION

Quantum dimer models[1,2] (QDM) provide simple examples[3,4] of microscopic Hamiltonians with short-ranged resonating valence-bond ground states (or dimer liquid) with gapped excitations and no broken symmetry ($\mathbb{Z}_2$ liquids). It has been known for a long time that such liquids are characterized by topological order;[5] although the system breaks no symmetry and has no local order parameter, the ground state acquires a degeneracy (in the thermodynamic limit) that depends on the genus of the surface where the model is defined (disk, cylinder, torus, etc.). Remarkably, such a topological degeneracy is insensitive to small, local perturbations (such as weak disorders, for instance).[6–8] On the other hand, it is clear that strong-enough local perturbations should lift this degeneracy. Consider, for instance, a $\mathbb{Z}_2$ dimer liquid on a cylinder, with a twofold, degenerate ground state. We turn on an external potential that penalizes (with an energy $\lambda > 0$) any dimer sitting across a line extending from one edge of the cylinder to the other. For very large λ, one effectively "cuts" the cylinder down to a disk topology, and one expects a single, nondegenerate ground state. It is therefore natural to expect a phase transition at some intermediate value λ.

We provide here a simple model where the spectrum, and the ground state degeneracy in particular, can be *exactly* calculated as a function of λ and the system size. This model generalizes a QDM on the kagome lattice (network of corner-sharing triangles with triangular and hexagonal plaquettes, see Fig. 1) that was introduced recently.[4] The full spectrum (and wave functions) can be obtained in an elementary way, and the excitations consist of static and noninteracting Ising vortices[9] (visons[10]). In this paper we show how the solution of the model extends to a situation where an external potential is applied along a line of the system. The solution is obtained by noting that the bulk of the system decouples from the line, and the line is exactly described by an Ising chain in transverse field (ICTF). As a result, we find a finite *critical* value λ_c of the perturbation below which the system behaves as a cylinder. (The energy difference between the two quasidegenerate ground states is exponentially small in the system size.) For $\lambda > \lambda_c$ the system behaves as a disk and the ground state is separated from the first excited state by a finite gap $\mathcal{O}(\lambda - \lambda_c)$.

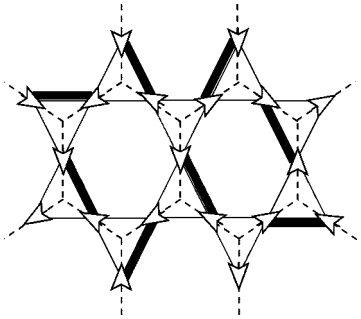

FIG. 1. A dimer covering on the kagome lattice (fat bonds). The corresponding representation with arrows living on the bonds of the hexagonal lattice (dashed lines) is displayed.

It has been argued that gapped systems with a topological degeneracy could provide physical ways to implement quantum bits (qubits) that would be protected from decoherence by their topological nature.[6,7,11,12] Since no *local* measurement can distinguish the different ground states if the system is infinitely large, any manipulation (unitary rotation) or measurement (projection) of the state of the qubit through local observables will have to rely on finite-size effects. We discuss this issue in Sec. V in light of the present solvable model. The effective Hamiltonian acting on the two lowest levels is expressed in terms of two generators T^x and T^z of rotations of the qubit about two quantization axes. We finally explain how one could take advantage of the phase transition at $\lambda=\lambda_c$ to perform unitary rotations. The problems of this approach, such as thermal excitations, will also be discussed briefly.

II. ARROW REPRESENTATION, SOLVABLE QDM, AND TOPOLOGICAL DEGENERACY

We consider a QDM defined on a kagome lattice with periodic boundary conditions in one direction (cylinder), but the arguments are easily generalized to other topologies.

A. Arrow representation

Because it is the natural formalism to describe and solve the QDM discussed here, we begin by reminding the representation of dimer coverings of the kagome lattice in terms of *arrows*.[4,13]

The sites of a kagome lattice K (noted i) can be identified with bonds of the hexagonal lattice H.[14] The triangles of K (noted t) are sites of H. As for hexagons of K (noted h), they also correspond to hexagons of H.

From a (fully packed) dimer covering of K we orientate the bonds of H (arrows) in the following way: Each bond of H is a site of K, which has one dimer, and the corresponding arrow points toward the interior of the triangle (of K) where the other end of the dimer is located. This is illustrated in Fig. 1. As a consequence, the number of incoming arrow(s) is even (0 or 2) at each vertex of H. Inversely, any arrow configuration satisfying the parity constraint at each vertex defines a unique dimer covering.

We can now define the operators τ^x, τ^z, and σ^x acting on the arrows. The notations are those of Refs. 4 and 15.

(i) τ_i^z: flips the arrow at site $i \in K$. Any product $\tau_i^z \tau_j^z \cdots$ around a *close loop* (of H) is a "physical" operator in the sense that it conserves all the constraints.

(ii) $\sigma_h^x = \Pi_{i=1}^6 \tau_i^z$. Flips the six arrows $i=1\cdots6$ around the hexagon h (smallest closed loop on H).[16] From the definition of τ^z above, the σ^x operators satisfy $(\sigma^x)^2=1$ and commute with each other.

(iii) τ_i^x: Compares the arrow at site i with the arrow in some (arbitrary) reference covering ($=+1$ if they are the same, -1 otherwise). The hard-core constraint on dimers translates into $\tau_0^x \tau_1^x \tau_2^x = 1$ for every triangle (012) of the kagome lattice.

From now on, and for most purposes, one can forget the dimers themselves and focus only on the bond degrees of freedom $\tau_i^x = \pm 1$.[17] We note that, in principle, the $\tau_i^x = \pm 1$ degrees of freedom could be physically realized with real spins living on a kagome lattice. A strong easy-axis anisotropy could then force them to point toward the center of one of the neighboring triangles.

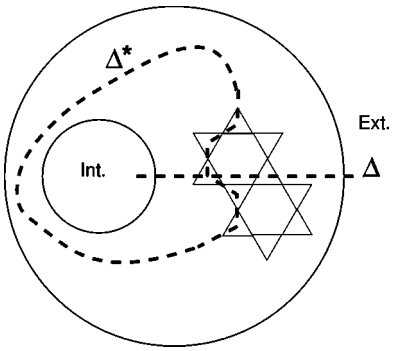

FIG. 2. Kagome lattice on a cylinder with a cut Δ going from one edge of the cylinder to the other. The dual cut Δ^* passes through the centers of the triangles and winds around the cylinder.

B. Bulk Hamiltonian

The QDM introduced in Ref. 4 is

$$\mathcal{H}_0 = -\sum_h \sigma_h^x = -\sum_h \prod_1^6 \tau_{h_i}^z. \tag{1}$$

All the eigenstates are easily obtained, because the σ_h^x operators commute with each other and have two eigenvalues $\sigma_h^x = \pm 1$.[18]

C. Topological sectors

As usual for dimer models, the configurations are grouped in topological sectors (TS); two configurations are in the same TS if and only if they can be transformed into each other by a succession of *local*[19] moves. As explained below, there are two TS when the system has the topology of a cylinder.

First, draw a cut Δ (crossing the bonds of the lattice) going from one edge of the cylinder to the other (Fig. 2). Let N_Δ be the number of dimers crossing Δ. It has a simple expression in terms of the τ_i^x,

$$N_\Delta = \frac{1}{2}\sum_{i=0}^{L} (1 - \tau_i^x), \tag{2}$$

where the sites $i=0\cdots L$ are the centers of the bonds of H that are cut by Δ, as shown in Fig. 3. For simplicity, we assume in Eq. (2) that no dimer crosses Δ in the reference covering.

Any *local* dimer move conserves the parity of N_Δ, and it is natural to define

$$T^x = \prod_{i \in \Delta} \tau_i^x = (-1)^{N_\Delta}. \tag{3}$$

All coverings with $T^x=1$ (-1) define a TS called S_+ (S_-) and $\mathcal{H}_0$ can be diagonalized separately in each sector.

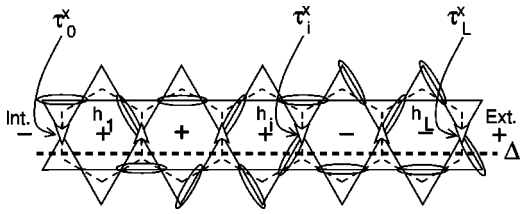

FIG. 3. Dimer covering of the kagome lattice in the vicinity of the cut Δ (dashed line). The arrows next to Δ [appearing in Eq. (2)] are shown. The signs in the hexagons Int., $h_1,\ldots,h_L$, Ext. indicate the values of the corresponding pseudospins σ^z (with the assumption that the reference configuration has no dimer crossing Δ).

D. Topological degeneracy of $\mathcal{H}_0$

It is straightforward to check that $\mathcal{H}_0$ has the same energy in each sector. Let Δ^* be a closed loop encircling the cylinder (Fig. 2), and define an operator,

$$T^z = \prod_{i\in\Delta^*} \tau_i^z, \tag{4}$$

that flips all the corresponding arrows. T^z commutes with all the σ^x operators and maps S_+ onto S_-,

$$T^z T^x = -T^x T^z \tag{5}$$

This shows that if $|\psi\rangle$ is an eigenstate of $\mathcal{H}_0$, $T^z|\psi\rangle$ is an eigenstate of $\mathcal{H}_0$ with the same energy (but in the other TS). This demonstrates the twofold (topological) degeneracy of the eigenstates of $\mathcal{H}_0$.

III. PERTURBATION LIFTING THE DEGENERACY BETWEEN THE $T^x=\pm 1$ SECTORS

We introduce a potential-energy term that couples to the dimers crossing Δ,[20]

$$\mathcal{H}_1 = 2\lambda N_\Delta \tag{6}$$

$$= \lambda \sum_{i=0}^{L} (1-\tau_i^x). \tag{7}$$

As discussed in the Introduction, we expect that a small λ should not affect the twofold degeneracy, while $\lambda \gg 1$ should leave a single ground state. In presence of $\mathcal{H}=\mathcal{H}_0+\mathcal{H}_1$, $T^x=(-1)^{N_\Delta}$ is still a conserved quantity, but T^z does not commute with $\mathcal{H}_1$, and the two sectors are no longer degenerate when $\lambda\neq 0$. Since for $\lambda\gg 1$ the system minimizes N_Δ, the ground state of the $T^x=+1$ sector tends to a state with $N_\Delta\simeq 0$ and that of the $T^x=-1$ sector to a state with $N_\Delta\simeq 1$. Instead of having a superposition of dimer configurations with different values of N_Δ, but a fixed *parity* (*nonlocal* observable), the large λ limit corresponds to a well-defined N_Δ (sum of *local* operators). While T^x is still a conserved quantity, we already see that the topological nature of the $T^x=+1$ and $T^x=-1$ sectors disappears when λ is large.

The perturbation $\mathcal{H}_1$ is identical to the one used by Ioffe *et al.*[7] in a triangular-lattice QDM in order to manipulate ("phase shifter") their qubit. However, in our case, *the existence of an arrow representation makes it possible to exactly calculate the spectrum* of $\mathcal{H}=\mathcal{H}_0+\mathcal{H}_1$.

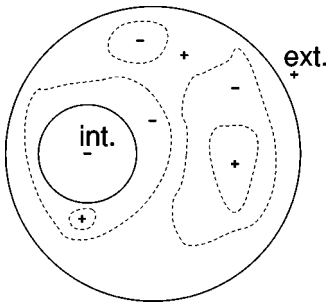

FIG. 4. Cylinder (full lines) and loops (dashed lines) along which a dimer configuration c differs from the reference. The signs indicate the value of σ^z in each domain.

A. Mapping to the ICTF

The Hamiltonian $\mathcal{H}=\mathcal{H}_0+\mathcal{H}_1$ [Eqs. (1) and (7)] can be separated into "bulk" and "chain" parts as below,

$$\mathcal{H} = \mathcal{H}_\Delta + \mathcal{H}_{\text{bulk}}, \tag{8}$$

$$\mathcal{H}_\Delta = -\sum_{i=1}^{L} \sigma_{h_i}^x + \lambda \sum_{i=0}^{L} (1-\tau_i^x), \tag{9}$$

$$\mathcal{H}_{\text{bulk}} = -\sum_{h'\notin\Delta} \sigma_{h'}^x. \tag{10}$$

It is important to emphasize that $\mathcal{H}_\Delta$ and $\mathcal{H}_{\text{bulk}}$ *commute with each other* and can therefore be treated separately. From now on we concentrate on $\mathcal{H}_\Delta$.

σ^z pseudospins—A σ_h^z operator can be introduced for each hexagon h in the following way. Due to the local constraint ($\tau_i^x\tau_j^x\tau_k^x=1$ on each triangle of K), the bonds of H where $\tau^x=-1$ necessarily form nonintersecting closed loops.[21] We interpret these loops as domain walls for some Ising pseudospins $\sigma_h^z=\pm 1$ that leave on each hexagon. To remove the twofold ambiguity we assume that the exterior has a fixed spin $\sigma_{\text{ext}}^z=1$. In turn, this defines a σ_{int}^z associated with the "interior" (Fig. 4). It is easy to check that this Ising spin labels the TS of the configuration because $\sigma_{\text{int}}^z=\Pi_{i\in\Delta^*}\tau_i^x=T^x$. The other bulk pseudospins are those introduced by Elser and Zeng.[13] Eventually we mention that σ_h^z and σ_h^x anticommute (they commute if not on the same hexagon), as suggested by the Pauli matrix notation. This is easily checked from the definition of σ_h^x in terms of arrows. From the definition of σ_h^z we have the relation,[4,22]

$$\sigma_h^z\sigma_{h'}^z = \tau_i^x, \tag{11}$$

where h and h' are the two hexagons touching i. For an arrow i_0 next to a boundary (say interior), this relation is modified to

$$\sigma_h^z\sigma_{\text{int}}^z = \tau_{i_0}^x. \tag{12}$$

These relations are used to get

$$\mathcal{H}_\Delta = -\sum_{i=1}^{L} \sigma^x_{h_i} - \lambda \sum_{i=0}^{L} \sigma^z_{h_i}\sigma^z_{h_{i+1}} + (L+1)\lambda, \qquad (13)$$

where the two boundary spins are identified as $\sigma^z_0 = \sigma^z_{\rm int}$ and $\sigma^z_{h_{L+1}} = \sigma^z_{\rm ext}$. It appears that $\mathcal{H}_\Delta$ is nothing but the Hamiltonian of an open ICTF with a magnetic exchange λ and a transverse field equal to 1. This model can be solved by a standard Jordan-Wigner transformation, and it maps onto free fermions. In the thermodynamic limit it has a paramagnetic phase with $\langle\sigma^z_h\rangle = 0$ for $|\lambda| < \lambda_c = 1$ and an ordered phase with $\langle\sigma^z_h\rangle \neq 0$ for $|\lambda| > \lambda_c = 1$.

The boundary spins σ^z_0 and $\sigma^z_{h_{L+1}}$ play special roles. $\sigma^z_{h_{L+1}} = \sigma^z_{\rm ext}$ is fixed to 1, but $\sigma^z_0 = \sigma^z_{\rm int}$ is free (but conserved by $\mathcal{H}_\Delta$) and labels the TS. The spectrum of the ICTF can thus be studied separately for $\sigma^z_0 = +1$ or $\sigma^z_0 = -1$. One takes $\lambda \geqslant 0$ (ferromagnetic chain) without loss of generality. The sector with $\sigma^z_0 = +1$ thus corresponds to *unfrustrated boundary conditions* for the (pseudospin) chain. On the other hand, choosing $\sigma^z_0 = -1$ amounts to imposing at least one Ising domain wall in the system.[23] In the thermodynamic limit both sectors have the same energy *per site*, but they may have a finite difference in the total energy (gap). In the paramagnetic phase ($\lambda < 1$), because of the finite spin-spin correlation length $\xi(\lambda)$, the frustration has an exponentially smaller effect on the ground-state energy, and the energy difference between the two TS is $\Delta E \sim \exp(-L/\xi)$ with $\xi \simeq \ln(1/\lambda)^{-1}$ (see Ref. 12 and Appendix A). On the other hand, in the ferromagnetic phase ($\lambda > 1$), the Ising spins want to order and the boundary condition $\sigma^z_0 \neq \sigma^z_L$ generates a *finite energy* cost $\Delta E \sim \mathcal{O}(L^0)$ [see Eq. (A13)].

The result is thus that for $\lambda < 1$ the ground state is asymptotically twofold degenerate in the thermodynamic limit. The gap between the two TS is $\Delta E \sim \exp[-L/\xi(\lambda)]$ where ξ is the correlation length of the ICTF. In the thermodynamic limit there is a finite critical value $\lambda_c = 1$, above which the topological degeneracy is destroyed. Above λ_c the Ising pseudospins have a positive magnetization. Since σ^z_h is an operator that creates an Ising vortex (vison[4]), it is natural to interpret $\langle\sigma^z_h\rangle > 0$ as the existence of a *condensate* of those particles (along Δ). This condensation is responsible for changing the "effective" topology of the system from a cylinder into a disk. In this simple model what happens along the chain Δ is decoupled from the bulk of the system. The perturbation caused by the potential λ does not extend into the bulk, which remains a liquid with noninteracting and static vison excitations.

IV. MIXING THE $T^x = \pm 1$ SECTORS WITH MONOMERS

The perturbation $\mathcal{H}_1$ discussed in Sec. III is not the only way to remove the topological degeneracy. It is well known that in the presence of mobile monomers, $T^x = (-1)^{N_\Delta}$ is no longer conserved.[24] This property was used in Refs. 7 and 11 to mix the topological sectors. We will show that in our kagome geometry the arrow representation of the dimer model allows us to exactly compute the spectrum of the system when monomers are allowed to be created, to hop, and to be destroyed along a line winding around the cylinder. As we will see, this model is closely related to the one discussed in the Sec. III: Δ is replaced by Δ^*, monomers will play the role of the visons, and the ICTF will have periodic and antiperiodic boundary conditions, instead of open ones.

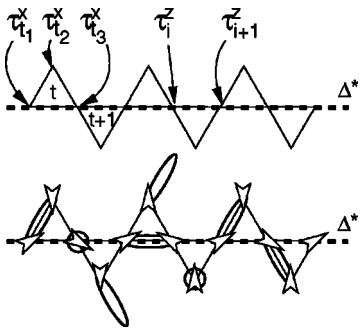

FIG. 5. Top: Kagome lattice in the vicinity of the cut Δ^* (dashed line). Bottom: Mixed dimer-monomer configuration and the arrow representation.

A. Hamiltonian

We relax the parity constraint $\tau^x_{t_0}\tau^x_{t_1}\tau^x_{t_2} = 1$ on each triangle t, so that triangles with one or three incoming arrows are allowed. When a triangle has *one* incoming arrow, it is naturally interpreted as the presence of a monomer (or hole) at the site of this arrow (see Fig. 5). When a triangle has *three* incoming arrows, we interpret it as a monomer and a dimer, which are delocalized over the three sites.[25] Flipping one arrow (i.e., acting with τ^z_i) on a dimer state therefore creates two monomers on the nearby triangles (one of which may be delocalized over three sites). We consider the following Hamiltonian:

$$\mathcal{H}'_0 = -\sum_h \sigma^x_h + U\sum_t (1 - \tau^x_{t_0}\tau^x_{t_1}\tau^x_{t_2}) \qquad (14)$$

$$= -\sum_h \prod_{i=1}^{6} \tau^z_{h_i} + U\sum_t (1 - \tau^x_{t_0}\tau^x_{t_1}\tau^x_{t_2}), \qquad (15)$$

where $h_{1\cdots6}$ are the sites around hexagon h, and $t_{1,2,3}$ are the sites of the triangle t (see Fig. 5). U is a large energy enforcing the constraint on low-energy states. This type of model was first considered by Kitaev.[6] For $U > 0$ the ground state of the Hamiltonian [Eq. (15)] is the same as for $U = \infty$ [equivalent to Eq. (1)] since $\tau^x_{t_0}\tau^x_{t_1}\tau^x_{t_2}$ commutes with all the σ^x. However, static pairs of monomers are present in excited states with energies greater than $2U$ above the ground state.

Like Ioffe and co-workers,[7,11] we wish to use these monomers to couple the two TS. For this purpose the monomers are allowed to be created and to propagate along one closed loop Δ^* winding around the cylinder (Fig. 2). The simplest term which does this is

$$\mathcal{H}'_1 = -\mu U \sum_{i\in\Delta^*} \tau^z_i. \qquad (16)$$

(This choice of normalization will make the analogy with the λ perturbation clearer.) When a τ^z_i term acts on a site located

between two triangles satisfying the constraint ($\tau^x_{t_0}\tau^x_{t_1}\tau^x_{t_2}=1$), it creates a pair of monomers. When it acts on a pair of triangles violating the constraint, the pair of monomers is destroyed. If it acts on a site located between triangles with different values of $\tau^x_{t_0}\tau^x_{t_1}\tau^x_{t_2}$, a monomer hops from one triangle to the other.

B. Mapping to the ICTF

As in Eq. (8), $\mathcal{H}'_0+\mathcal{H}'_1$ splits into bulk and one-dimensional parts,[26]

$$\mathcal{H}'_0+\mathcal{H}'_1=\mathcal{H}'_{\text{bulk}}+\mathcal{H}_{\Delta^*}, \tag{17}$$

$$\mathcal{H}'_{\text{bulk}}=-\sum_h \sigma^x_h+U\sum_{t\notin\Delta^*}(1-\tau^x_{t_0}\tau^x_{t_1}\tau^x_{t_2}), \tag{18}$$

$$\mathcal{H}_{\Delta^*}=-\mu U\sum_{i\in\Delta^*}\tau^z_i+U\sum_{t\in\Delta^*}(1-\tau^x_{t_0}\tau^x_{t_1}\tau^x_{t_2}). \tag{19}$$

One can simply check that $\mathcal{H}_{\Delta^*}$ and $\mathcal{H}'_{\text{bulk}}$ commute with each other, so that one has to study a one-dimensional model $\mathcal{H}_{\Delta^*}$. This model is identical to a closed ICTF (with periodic or antiperiodic boundary conditions), as explained below. Each *triangle* t crossed by Δ^* corresponds to a *site* of the spin chain. The associated transverse-field term for this Ising spin is

$$\tilde{\sigma}^x_t=\tau^x_{t_0}\tau^x_{t_1}\tau^x_{t_2}. \tag{20}$$

We define the z component of the spins as

$$\tilde{\sigma}^z_t=\tau^z_0\tau^z_1\cdots\cdots\tau^z_{i(t)}, \tag{21}$$

where 0 is an (arbitrary) origin on Δ^* and $i(t)$ is the site of K in common with triangles t and $t-1$. It is simple to check that the $\tilde{\sigma}^x$ and $\tilde{\sigma}^z$ defined above (not to be confused with σ^x and σ^z) obey the usual Pauli matrix algebra and play the role of spin-$\frac{1}{2}$ operators. In addition, these definitions ensure that

$$\tilde{\sigma}^z_t\tilde{\sigma}^z_{t+1}=\tau^z_{t_3}, \tag{22}$$

where t_3 is the common site between triangles t and $t+1$ (as in Fig. 5). Because Δ^* is a closed curve, special care is needed for the last term,

$$T^z\tilde{\sigma}^z_{L-1}\tilde{\sigma}^z_0=\tau^z_0, \tag{23}$$

where T^z [defined in Eq. (4)] commutes with $\mathcal{H}_{\Delta^*}$ (in the same way as before with $[\mathcal{H}_\Delta,T^x]=0$). It can be successively set to ±1 to obtain the whole spectrum. With these notations $\mathcal{H}_{\Delta^*}$ reads

$$\frac{1}{U}\mathcal{H}_{\Delta^*}=-\mu\left(T^z\sigma^z_{L-1}\tilde{\sigma}^z_0+\sum_{t=0}^{L-2}\tilde{\sigma}^z_t\tilde{\sigma}^z_{t+1}\right)-\sum_{t=0}^{L-1}\tilde{\sigma}^x_t+\text{cst}. \tag{24}$$

This is the Hamiltonian of an ICTF with periodic boundary conditions when $T^z=1$ and with antiperiodic boundary conditions when $T^z=-1$. As for $\mathcal{H}_\Delta$, the model has, in the thermodynamic limit, a phase transition at $\mu_c=1$ between a paramagnetic phase and a ferromagnetic phase. The calculation of the gap between the two sectors amounts to studying a closed ICTF with periodic and antiperiodic boundary conditions. The exact result for the energy difference $\Delta E'$ is derived in Appendix B (see also Ref. 12) with the help of a Jordan-Wigner transformation. In the limit of a large system ($L\gg1$) it is given by

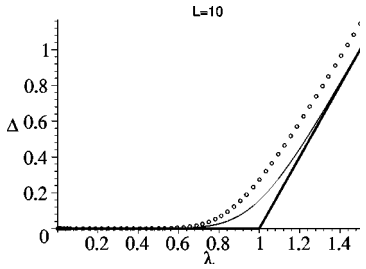

FIG. 6. Effect of a change of boundary conditions on the ground-state energy of an ICTF with $N=10$ spins as a function of the (ferromagnetic) exchange λ. Circles: closed chain with periodic and antiperiodic boundary conditions. Thin line: ground-state energy difference between open chain with ferromagnetic ($\uparrow\cdots\uparrow$) and antiferromagnetic ($\downarrow\cdots\uparrow$) boundary conditions. Thick line: $N=\infty$ case (same result for the open and closed chains).

$$\Delta E'=E_+-E_-\simeq 2U\sqrt{\frac{1-\mu^2}{L\pi}}\mu^L \quad \text{for} \quad \mu<1 \tag{25}$$

$$\simeq 2U(\mu-1) \quad \text{for} \quad \mu>1. \tag{26}$$

The result for $L=10$ is plotted in Fig. 6. As for $\mathcal{H}_\Delta$, the critical value $\mu_c=1$ separates a regime with an exponentially small splitting between the sectors [Eq. (25)] and a regime with a finite gap between them [Eq. (26)]. In the spin language, the ferromagnetic phase is characterized by $\langle\tilde{\sigma}^z\rangle\neq0$. Going back to dimer and monomers variables, we find that $\tilde{\sigma}^z_t$ flips all the arrows located on Δ^* between the origin and t. Thus, it creates or annihilates a pair of monomers sitting at both ends of the string or moves a monomer from one end to the other. In both cases $\tilde{\sigma}^z_t$ creates or destroys a monomer on the triangle t.[26] $\langle\tilde{\sigma}^z\rangle\neq0$ can thus be interpreted as a *condensation* of monomers along Δ^*. This is equivalent to the condensate of visons mentioned in the case of $\mathcal{H}_\Delta$ when $\lambda>1$.

To conclude this section we discuss a difference between the λ and the μ perturbations. In the limit where $\lambda\to\infty$ no dimer can sit on Δ anymore and the torus is reduced to a rectangle, as if the lattice had been cut with scissors. If the same geometrical picture was true for the perturbation μ along Δ^*, one would erroneously conclude that the system is effectively transformed into *two* cylinders with a fourfold ground state degeneracy. This is incorrect for the following reason. The path Δ^* chosen to define $T^z(\Delta^*)$ [Eq. (4)] may be shifted by multiplication with a σ^x operator,

$$\sigma^x(h)T^z(\Delta^*_1)=T^z(\Delta^*_2), \tag{27}$$

where h is a hexagon next to Δ^*_1 and Δ^*_2 is identical to Δ^*_1, except that it passes on the other side of h. From Eq. (27), we see that $T^z(\Delta^*_1)|0\rangle$ does not depend on the location of Δ^*_1, as long as this closed curve is deformed by passing only on

hexagons with $\sigma^x(h)=1$. In the case of a perturbation μ, the ground state satisfies $\sigma^x(h)|0\rangle=|0\rangle$ for all hexagons h, even those along Δ^*. (This is not true for the λ perturbation which does not commute with σ^x.) Therefore, one cannot independently flip the topological sector of the "upper" cylinder with some T_1^z without changing the sector of the "lower part," which is controlled by a T_2^z, since $T_1^z|0\rangle=T_2^z|0\rangle$.

V. A TOY MODEL FOR A TOPOLOGICAL QUBIT

Kitaev[6] suggested that systems with topologically degenerate ground states could be used to realize qubits protected from decoherence. This suggestion was then made more precise by Ioffe and co-workers[7,11] and Douçot and co-workers[12,28] who proposed to use Josephson junctions arrays to implement such a system. As mentioned in the Introduction, the topological nature of the degeneracy makes it difficult to "manipulate" (perform unitary rotation), because it is almost insensitive to local couplings. On the other hand, it may be difficult to apply a perturbation corresponding to a nonlocal operator (such as T^z or T^y). If, however, the system allows for a hardware implementation of such a nonlocal operator,[29] it represents a dangerous channel through which perturbations could bypass the topological protection and contribute to the decoherence of the qubit. If such a nonlocal coupling to the system exists, one must be able to "disconnect" it efficiently when it is not active.

The clever solution proposed in Refs. 7 and 11 consists of perturbing the system with two external potentials acting along two lines, exactly like Δ and Δ^*. While these perturbations are local (more precisely they are sums of local terms), they induce a splitting of the two ground states proportional to λ^L and therefore induce a slow precession of the qubit. In this section we take advantage of the exact solution of the model to discuss these effects beyond the regime where $\lambda^L \ll 1$.

A. Unitary rotations

Combining the perturbations along Δ and Δ^* the Hamiltonian is

$$\mathcal{H}(\lambda,\mu) = \mathcal{H}_{0'} + \mathcal{H}_{1'} + \mathcal{H}_1$$

$$= -\sum_h \prod_{i=1}^{6} \tau^z_{h_i} + U\sum_t (1-\tau_0^x\tau_1^x\tau_2^x) \qquad (28)$$

$$-\mu U \sum_{i\in\Delta^*} \tau_i^z - \lambda \sum_{i\in\Delta} (\tau_i^x - 1). \qquad (29)$$

From the previous calculations we know that $\mathcal{H}(\lambda,\mu=0)$ lifts the degeneracy of the two TS. It acts in this two-dimensional subspace as $\Delta E(\lambda)T^x$, where $\Delta E(\lambda)$, given in Eqs. (A13) and (A15), is the energy difference between the ferromagnetic and antiferromagnetic boundary conditions for an ICTF with exchange λ (and a unit transverse field). On the other hand, $\mathcal{H}(\lambda=0,\mu)$ mixes the two sectors. Its action is described by $U\Delta E'(\mu)T^z$ where $\Delta E'$ [Eq. (B23)] is the energy difference between the periodic and antiperiodic boundary conditions for an ICTF (with exchange μU and transverse field U).[30]

If the system is operated below the critical values of λ and μ, the qubit precesses at a frequency that is exponentially small in the system size. The cylinder topology and the low density of monomers protect the degeneracy of the spectrum. This is the regime mentioned by Ioffe and co-workers. However, the system size cannot be too large, because the time required for a unitary rotation would become exponentially long. On the other hand, if the system is not large enough, its topology does not fully protect it from decoherence by external perturbations.

If one of the external parameters (λ or μ) is pushed above its critical value, the frequency becomes finite, even in case of a large system size. We may therefore take advantage of the phase transitions in a large system. In such a case the qubit is topologically protected as long as λ and μ are smaller than their critical values, even if they are not precisely set to zero or if they introduce some noise. It is only during the manipulation [$\lambda(t)>1$ or $\mu(t)>1$] that the state of the qubit evolves (and is sensitive to the external noise entering through Δ or Δ^*).

To preserve an adiabatic evolution one must avoid transitions to other eigenstates. However the gap in the spectrum of the ICTF becomes small (of the order of $\sim 1/L$) in the vicinity of the transition. This limits the typical time of the unitary rotation to be at least of the order of L. This *linear* dependence in the system size is an interesting property, because it should be compared to the *exponential* dependence ($\sim\lambda^{-L}$) present in the perturbative regime. Also because of this small gap, the temperature must be $T \ll 1/L$ to avoid thermal excitations when λ (or μ) is close to 1. Using the transition to perform unitary rotation, therefore, seems to improve the time of operation and could enable us to use a larger system and benefit from a stronger topological protection. It also requires us to work at a lower temperature than that for a qubit operated in the perturbative ($\lambda,\mu \ll 1$) regime only, and this may represent a severe limitation.

B. Reading out the state of the qubit

We assume that the qubit is in a linear combination of the two topological sectors, $|\psi\rangle=\alpha|+\rangle+\beta|-\rangle$ where $T^x|+\rangle=|+\rangle$ and $T^x|-\rangle=-|-\rangle$. We wish to measure $|\alpha|^2$ with a *local* observable. This is not directly possible if the system is very large, since any local observable has expectation values in $|+\rangle$ and $|-\rangle$, which are exponentially close. Likewise, a local observable has a vanishing matrix element between $|+\rangle$ and $|-\rangle$. A possible procedure could be to switch adiabatically the potential λ above the transition. For a strong-enough λ, the state $|+\rangle$ evolves to a superposition of dimer coverings with no dimer crossing Δ. On the other hand, $|-\rangle$ evolves to a superposition of dimer coverings with *one* dimer crossing Δ. This is because the parity (T^x) is a conserved quantity under the evolution, but the ground state has to minimize N_Δ as $\lambda(t)$ grows. A (projective) measurement detecting the presence of a dimer on some bond crossing Δ will thus give 1 with the probability $|\alpha|^2/L$. The whole operation has to be repeated many times ($\sim L$) before $|\alpha|^2$ is known with a rea-

sonable accuracy, but one may improve the efficiency of the measurement by having a bond along Δ, where the energy cost of a dimer is less than on other bonds (in which case the dimer, if present, will localize on this particular bond when λ becomes large). Of course the reading procedure described above suffers from the same limitations (time proportional to L and low temperature) as the unitary rotation.

VI. CONCLUSIONS

We have shown that the QDM of Eq. (1) can be simply solved in the presence of two kinds of perturbations: an external potential that couples to dimers crossing a line or the inclusion of monomers. This provides a simple example of system with a $\mathbb{Z}_2$ fractionalized phase, where the topological degeneracy is destroyed by tuning an external parameter through a quantum phase transition (belonging to the classical Ising two-dimensional (2D) universality class).

We also discussed some properties of this toy model from the point of view of an ideal topological qubit, in which case the exact solution allows us to follow the two lowest eigenstates as a function of some external parameters. These two parameters can be used to perform unitary rotations of the qubit and provide an exactly solvable version of some ideas introduced previously.[7] In addition, we pointed out that the phase transition could, in principle, be used to improve the robustness to decoherence, because it could enable us to use a larger (although not infinite) system. Concerning the measurement of the qubit, we also emphasize the interesting properties of the phase transition as it turns a nonlocal property (*parity* of the number of dimers crossing a line) into a local property (dimer *density*). From this point of view, we note that the method has some resemblance to the flux-trapping experiment imagined by Senthil and Fisher[10] to detect visons in $\mathbb{Z}_2$ fractionalized systems.

ACKNOWLEDGMENTS

We thank Benoît Douçot for stimulating discussions. G. M. is in part supported by the Ministère de la Recherche et des Nouvelles Technologies with an ACI grant, and he acknowledges the hospitality of IRRMA.

APPENDIX A: GROUND-STATE ENERGY OF AN ICTF WITH OPEN BOUNDARY CONDITIONS

We apply fixed boundary conditions to an open ICTF and compute the energy difference between those for the cases of ferromagnetic boundary conditions (two fixed up-spins at the ends) and antiferromagnetic boundary conditions (one up-spin at one end and a down-spin at the other). This result was obtained recently by Douçot *et al.*,[12] but we give here for completeness a detailed derivation of the result.

1. Hamiltonian and free fermions

The Hamiltonian is

$$\mathcal{H} = -\sum_{n=1}^{L} \sigma_n^x - \mu \sum_{n=0}^{L} \sigma_n^z \sigma_{n+1}^z, \tag{A1}$$

with two fixed spins at the ends of the chain, $\sigma_{L+1}^z = 1$ and $\sigma_0^z = \pm 1$, depending on the boundary conditions. Using a standard Jordan-Wigner transformation to represent the Ising operators with spinless fermions,

$$\sigma_n^x = 2c_n^\dagger c_n - 1, \tag{A2}$$

$$\sigma^y + i\sigma^z = 2c_n^\dagger \exp\left(i\pi \sum_{i=0}^{n-1} c_i^\dagger c_i \right), \tag{A3}$$

$$\sigma_n^z \sigma_{n+1}^z = (c_n^\dagger + c_n)(c_{n+1} - c_{n+1}^\dagger). \tag{A4}$$

$\mathcal{H}$ is quadratic in the fermion operators and can be diagonalized by a Bogoliubov transformation. To find the quasiparticle creation operators $d^\dagger$ we consider the following form (Ansatz):[31]

$$d_\omega^\dagger = f_\omega^\dagger - f_{\omega^{-1}}^\dagger, \tag{A5}$$

$$f_\omega^\dagger = \sum_{n=0}^{L+1} \omega^n (c_n^\dagger + c_n) + ib(\omega) \sum_{n=0}^{L+1} \omega^n (c_n^\dagger - c_n), \tag{A6}$$

where ω and $b(\omega)$ have to be determined. One can check that

$$[\mathcal{H}, d_\omega^\dagger] = E(\omega) d_\omega^\dagger,$$

$$[\mathcal{H}, d_\omega] = -E(\omega) d_\omega, \tag{A7}$$

with $E(\omega) \geqslant 0$, provided the following equations are satisfied:

$$E(\omega) = -2ib(\omega)(1 + \lambda\omega^{-1}), \tag{A8}$$

$$iE(\omega)b(\omega) = -2(1 + \lambda\omega), \tag{A9}$$

$$\omega^{L+1} - \omega^{-L-1} = -\lambda(\omega^{L+2} - \omega^{-L-2}). \tag{A10}$$

The two first equations come from the terms $0 \leqslant n \leqslant \mathrm{Lg}$ in Eq. (A7). These equations determine the energy of the quasiparticles as a function of ω,

$$E(\omega) = 2\sqrt{\lambda^2 + \lambda(\omega + \omega^{-1}) + 1}. \tag{A11}$$

The third equation (A10) comes from the boundary at $n = L+1$ and is a constraint on the available ω.

2. Case $\lambda \geqslant (L+1/L+2)$

For $\lambda \geqslant (L+1/L+2)$ the Eq. (A10) has $L+1$ distinct solutions of the form,

$$\omega = e^{ik} \quad \text{with} \quad k \in [0, \pi],$$

$$\lambda = -\frac{\sin[(L+1)k]}{\sin[(L+2)k]}. \tag{A12}$$

These fermionic levels are those required to describe the $L+1$ spins $n = 0 \cdots L$. Because we have chosen E to be always

positive, the absolute ground state (whatever σ_0^z) is the vacuum $|0\rangle$ of the $d_\omega^\dagger$. The lowest excited state is $d_{k_0}^\dagger|0\rangle$, where we have added the fermion with the smallest energy Δ. It corresponds to the solution k_0 of Eq. (A12), which is the closest to π. This solution can be calculated by an expansion in $1/L$ and we obtain

$$\Delta = 2(\lambda - 1) + \frac{\lambda \pi^2}{(\lambda - 1)L^2} + \mathcal{O}(L^{-3}). \tag{A13}$$

So far we have not specified the value of σ_0^z corresponding to each level. In the limit where $\lambda \gg 1$ it is clear that the ground state is in the sector $\sigma_0^z = 1$. Since one can show that no level crossing occurs for $\lambda > 0$ in such a finite chain, the fermion vacuum $|0\rangle$ satisfies $\sigma_0^z|0\rangle = |0\rangle$ for all $\lambda > 0$ and corresponds to a state of the system with ferromagnetic boundaries. On the other hand, inserting any $d_\omega^\dagger$ fermion changes the sign of σ_0^z (since all $d_\omega^\dagger$ anticommute with $\sigma_0^z = c_0^\dagger + c_0$). The first excited state $d_{k_0}^\dagger|0\rangle$ is thus the ground state of the system with antiferromagnetic boundary conditions ($\sigma_0^z = -1$), and the gap between the two sectors is given by Δ [Eq. (A13)].

3. Case $0 < \lambda \leqslant (L+1/L+2)$

In the range $0 > \lambda \geqslant (L+1/L+2)$, only L solutions of the form of Eqs. (A12) exist. The "missing" solution ω_0 has the lowest energy and is real, $\omega_0 \in]-\infty, 0]$. It corresponds to a bound state (imaginary wave vector) for the fermions. In the thermodynamic limit one has $\omega_0 = -1/L$ and finite-size corrections can be evaluated,

$$\omega_0 = -\frac{1}{L} + \lambda^{2L+1}(1 - \lambda^2) + \mathcal{O}(L\lambda^{4L}), \tag{A14}$$

which gives an energy gap,

$$\Delta = 2\lambda^{L+1}(1 - \lambda^2) + \mathcal{O}(L\lambda^{3L}). \tag{A15}$$

As before, this gap is the ground-state energy difference between antiferromagnetic and ferromagnetic boundary conditions for the spin chain.

APPENDIX B: GROUND-STATE ENERGY OF AN ICTF WITH PERIODIC OR ANTIPERIODIC BOUNDARY CONDITIONS

We compute the ground-state energy of a closed ICTF with periodic and antiperiodic boundary conditions. The latter result has also been obtained recently by Douçot *et al.*,[12] but we give here a detailed derivation of the result. We also note that this calculation has some similarities to the evaluation of the ground-state energy splitting in the triangular-lattice QDM at the Rokhsar-Kivelson point (using a Pfaffian technique).[8]

1. Periodic boundary conditions

The Hamiltonian is

$$\mathcal{H} = -\sum_{n=0}^{L-1} \sigma_n^x - \mu \sum_{n=0}^{L-1} \sigma_n^z \sigma_{n+1}^z, \tag{B1}$$

with $\sigma_L^z = \sigma_0^z$. The Ising operators are represented with spinless fermions, as in Eqs. (A2)–(A4). Due to the periodic boundary conditions we also have

$$\sigma_{L-1}^z \sigma_0^z = -(c_{L-1}^\dagger + c_{L-1})(c_0 - c_0^\dagger)\exp\left(i\pi \sum_{n=0}^{L-1} c_n^\dagger c_n\right). \tag{B2}$$

It is simple to check that

$$\prod_{n=0}^{L-1} \sigma_n^x = \exp\left(i\pi \sum_{n=0}^{L-1} c_i^\dagger c_i\right) \tag{B3}$$

is a conserved quantity. The spectrum can thus be studied separately in the sectors $\Pi_{n=0}^{L-1}\sigma_n^x = \pm 1$. However $\mathcal{H}$ has off-diagonal matrix elements in the natural Ising basis which are all $\leqslant 0$. This ensures that the ground state has only positive weight in this basis, and it therefore belongs to the sector

$$\prod_{n=0}^{L-1} \sigma_n^x = 1. \tag{B4}$$

In the following we thus consider fermions subjected to *antiperiodic boundary conditions* [see Eqs. (B3) and (B4) and the $-$ sign in the right-hand side of Eq. (B2)].

After Fourier transform the Hamiltonian becomes

$$\mathcal{H}_{\text{chain}} = \sum_{k=(2n+1)\pi/L} \{[i\mu \sin(k) c_k^\dagger c_{-k}^\dagger + \text{H.c.}] - 2c_k^\dagger c_k[\mu \cos(k) + 1] + 1\}, \tag{B5}$$

which is diagonalized by a Bogoliubov transformation,

$$\mathcal{H}_{\text{chain}} = \sum_{k=(2n+1)\pi/L} \epsilon(k)\left[d_k^\dagger d_k - \frac{1}{2}\right], \tag{B6}$$

$$\epsilon(k) = 2\sqrt{\mu^2 + 1 + 2\mu \cos(k)}. \tag{B7}$$

Using the explicit form of the transformation and the antiperiodic boundary conditions on the fermions, one can show that the vacuum $|0\rangle$ of the $d_k^\dagger$ fermions satisfies

$$\exp\left(i\pi \sum_{n=0}^{L-1} c_n^\dagger c_n\right)|0\rangle = +|0\rangle. \tag{B8}$$

This is consistent with Eq. (B4) and the ground state is thus $|0\rangle$. Its energy is

$$E_P = -\frac{1}{2} \sum_{k=(2n+1)\pi/L} \epsilon(k). \tag{B9}$$

2. Antiperiodic boundary conditions

To ensure that $\sigma_L^z = -\sigma_0^z$, the fermions are now subjected to *periodic* boundary conditions [see Eq. (B2)]. However, for $\mu > 1$ it is necessary to add one $d_k^\dagger$ fermion to ensure the

correct parity under a global spin flip. Since the dispersion relation $\epsilon(k)$ is minimum in $\epsilon(k=0)=2|\mu-1|$, the ground state for $\mu>1$ is

$$|1\rangle = d_0^\dagger|0\rangle. \tag{B10}$$

The ground-state energy of the chain with antiperiodic boundary conditions is thus

$$E_A = -\frac{1}{2}\sum_{k=(2n/L)\pi} \epsilon(k) + 2(\mu-1) \quad \text{for} \quad \mu>1 \tag{B11}$$

$$= -\frac{1}{2}\sum_{k=(2n/L)\pi} \epsilon(k) \quad \text{for} \quad 0\leqslant\mu\leqslant 1. \tag{B12}$$

3. Energy difference

From the calculation above the energy difference between the ground states of the two boundary conditions is (for $\mu \leqslant 1$)

$$E_A - E_P = \sqrt{2\mu}\sum_{n=0}^{L-1}\left[\sqrt{\cosh\alpha_0 - \cos(k_{n+1/2})} - \sqrt{\cosh\alpha_0 - \cos(k_n)}\right], \tag{B13}$$

where

$$k_n = \frac{2n\pi}{L}, \tag{B14}$$

and α_0 is defined by

$$\cosh\alpha_0 = \frac{\mu^2+1}{2\mu} (\geqslant 1), \tag{B15}$$

$$\alpha_0 = -\ln(\mu). \tag{B16}$$

The difference between the two sums can be related to a contour integral I_0 in the complex plane,

$$E_A - E_P = \sqrt{2\mu} L I_0, \tag{B17}$$

where

$$I_0 = -\frac{1}{2i\pi}\oint_C \frac{f(z)}{\sin(Lz)}dz, \tag{B18}$$

and

$$f(z) = \sqrt{\cosh\alpha_0 - \cos(z)}. \tag{B19}$$

The contour is shown Fig. 7. The equality, Eq. (B17), can be demonstrated by using the fact that the poles inside the contour are located at $z=k_n$ and $z=k_{n+1/2}$, and they have alternating residues proportional to $-f(k_n)/L$ and $+f(k_{n+1/2})/L$. The contour can be decomposed into several regions, $I_0=I_A+I_{A'}+I_B+I_C+I_{C'}$ (Fig. 7). Using the odd parity of the integrand

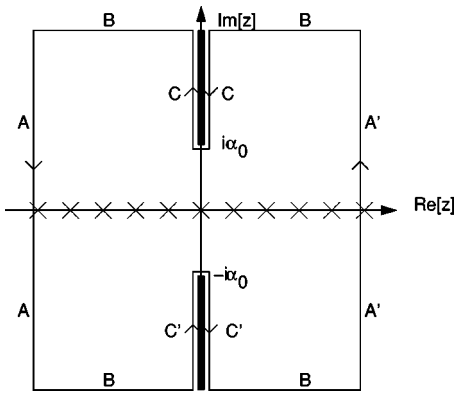

FIG. 7. Contour in the complex plane used to define the integral I_C. The crosses on the real axis indicate the poles of $1/\sin(Lz)$ and the fat segments on the imaginary axis indicate the branch cuts of $f(z)$. The region B is sent to $\mathrm{Im}[z]=\pm\infty$.

under $z\to -z$, one has $I_C=I_{C'}$, and using the periodicity under $z\to z+2\pi$ one finds $I_A+I_{A'}=0$. The integrand is exponentially small when $\mathrm{Im}[z]\to\pm\infty$, so the region B does not contribute. We therefore have $I_0=2I_C$. The integral over the region C is given by the discontinuity of the integrand along the branch cut,

$$I_C = \frac{1}{2i\pi}\int_{\alpha_0}^{\infty} idr\left\{\frac{f(ir+o^-)}{\sin[L(ir+o^-)]} - \frac{f(ir+o^+)}{\sin[L(ir+o^+)]}\right\} = \frac{1}{\pi}\int_{\alpha_0}^{\infty} dr\frac{\sqrt{\cosh(r)-\cosh(\alpha_0)}}{\sinh(Lr)}. \tag{B20}$$

When the system size is large ($L\to\infty$) the behavior of I_C is dominated by values of r close to α_0. In this limit,

$$I_C \simeq \frac{\sqrt{\sinh\alpha_0}}{\pi}\int_{\alpha_0}^{\infty} dr e^{-Lr}\sqrt{r-\alpha_0} \simeq \frac{\sqrt{\sinh\alpha_0}}{2\sqrt{\pi}} e^{-L\alpha_0} L^{-3/2}, \tag{B21}$$

so that the energy difference is

$$E_A - E_P = 2\sqrt{2\mu} L I_C \simeq 2\sqrt{\frac{2\mu\sinh\alpha_0}{L\pi}} e^{-L\alpha_0} \tag{B22}$$

$$\simeq 2\sqrt{\frac{1-\mu^2}{L\pi}}\mu^L. \tag{B23}$$

The calculation of E_A-E_P for $\mu>1$ is almost identical to the $\mu<1$ case described above. The difference between the sums of $\epsilon(k)$ on "even" and "odd" momenta is again expressed with the integral I_C, but with $\alpha_0=\ln(\mu)$. Combining this with Eqs. (B9) and (B11) gives

$$E_A - E_P = 2(\mu-1) + 2\sqrt{\frac{\mu^2-1}{L\pi}}\mu^{-L}. \tag{B24}$$

[1] D. S. Rokhsar and S. A. Kivelson, Phys. Rev. Lett. **61**, 2376 (1988).

[2] The configurations of a *classical* dimer model are subsets of lattice bonds in which every site is taken once. In other words, every site is occupied by exactly one dimer. In a *quantum* dimer model, these configurations form an orthonormal basis of the Hilbert space. The Hamiltonian generally has dimer hopping terms (kinetic energy) which allow $n \geqslant 2$ dimers to hop on empty bonds around closed loops of length $2n$. The Hamiltonian may also include diagonal (potential) terms that favor or penalize some particular local patterns. For a brief introduction to QDM, see, for instance, Sec. 5 of G. Misguich and C. Lhuillier. Review chapter published in the book *Frustrated spin systems*, edited by H. T. Diep, (World-Scientific, Singapore, (2005).

[3] R. Moessner and S. L. Sondhi, Phys. Rev. Lett. **86**, 1881 (2001).

[4] G. Misguich, D. Serban, and V. Pasquier, Phys. Rev. Lett. **89**, 137202 (2002).

[5] X. G. Wen, Phys. Rev. B **44**, 2664 (1991).

[6] A. Yu. Kitaev, Ann. Phys. (San Diego) **303**, 2 (2003).

[7] L. B. Ioffe, M. V. Feigel'man, A. Ioselevich, D. Ivanov, M. Troyer, and G. Blatter, Nature (London) **415**, 503 (2002).

[8] A. Ioselevich, D. A. Ivanov, and M. V. Feigelman, Phys. Rev. B **66**, 174405 (2002).

[9] N. Read and B. Chakraborty, Phys. Rev. B **40**, 7133 (1989); S. Kivelson *ibid.* **39**, 259 (1989).

[10] T. Senthil and M. P. A. Fisher, Phys. Rev. Lett. **86**, 292 (2001); Phys. Rev. B **63**, 134521 (2001).

[11] L. B. Ioffe and M. V. Feigel'man, Phys. Rev. B **66**, 224503 (2002).

[12] B. Douçot, M. V. Feigel'man, L. B. Ioffe, and A. S. Ioselevich, Phys. Rev. B **71**, 024505 (2005).

[13] V. Elser and C. Zeng, Phys. Rev. B **48**, 13647 (1993).

[14] In fact H can be any trivalent lattice (each site has three neighbors) with any topology: disk, sphere, cylinder, torus, etc. As an example, H can be a hexagonal lattice with periodic boundary conditions in one direction (cylinder). Then one constructs a new lattice K by medial lattice construction; sites of K are the middle points of the bonds of H (Ref. 32). In the following, for simplicity, we will choose H to be a hexagonal lattice and K to be a kagome lattice (hence, the names H and K).

[15] See also paragraph 5.6 of Ref. 2.

[16] In terms of dimers, σ_h^x is the sum of all possible "kinetic energy" terms (ring exchange) that can be defined inside the star surrounding h. Those terms allow from three to six dimers to move.

[17] Those bond variables are $\mathbb{Z}_2$ gauge degrees of freedom (Ref. 4), while the local constraint is the Gauss law of the gauge description (Ref. 33). As for $\sigma_h^x = \Pi_{i=1}^6 \tau_i^z$, it is the gauge flux going through the hexagon h.

[18] They are independent pseudospin operators. Notice, however, that if the system has no edge (torus or sphere), they are subjected to an additional constraint $\Pi_h \sigma^x(h) = 1$. This comes from the fact that, in such a geometry, $\Pi_h \sigma^x(h)$ flips every arrow *twice* and thus reduces to the identity.

[19] Here "local" means that the associated loop does not wind around the whole system (cylinder).

[20] The case where the potential term pins the dimers along some reference configuration in the *whole* system is discussed in Ref. 4 and is equivalent to a two-dimensional (2D) Ising model in a transverse field.

[21] These are bonds where the arrows have different orientations in c and in the reference.

[22] The relation between the τ and σ operators is the same as the standard duality between Ising models and $\mathbb{Z}_2$ gauge theory in $2+1$ dimensions. See Ref. 4.

[23] The relation between the topological sectors of QDM and the boundary conditions in spin models was already noted in Refs. 4, 33, and 34, together with the connection between confinement transition and Ising transition.

[24] If a monomer winds around the cylinder, it connects a configuration $T^x = 1$ with a configuration $T^x = -1$.

[25] In the $\mathbb{Z}_2$ gauge-theory language the constraint is the Gauss law and allowing triangles with $\tau_{t_0}^x \tau_{t_1}^x \tau_{t_2}^x = -1$ amounts to allowing gauge charges ("matter") in the system.

[26] U need not have the same value in the bulk and along Δ^*. One can also choose $U = \infty$ in the bulk and $U < \infty$ along Δ^*, so that monomers can exist and propagate only along the chain.

[27] This should be compared with σ_h^z, which creates a vison on hexagon h.

[28] B. Douçot, M. V. Feigel'man, and L. B. Ioffe, Phys. Rev. Lett. **90**, 107003 (2003).

[29] In the circuit proposed in Ref. 7, the state of the qubit could be measured through a weak Josephson junction connecting the two edges of the cylinder.

[30] Since any unitary operation can be performed using T^x and T^z sequentially, there is no need to analyze the spectrum with $\lambda \neq 0$ and $\mu \neq 0$ simultaneously.

[31] Eq. (A5) will ensure that $\sigma_0^z = c_0^\dagger + c_0$ do not appear in $d_\omega^\dagger$, so that $d_\omega^\dagger$ and d_ω anticommute with σ_0^z.

[32] See Sec. III of G. Misguich, D. Serban, and V. Pasquier, Phys. Rev. B **67**, 214413 (2003).

[33] R. Moessner, S. L. Sondhi, and E. Fradkin, Phys. Rev. B **65**, 024504 (2002).

[34] R. Moessner and S. L. Sondhi, Phys. Rev. B **68**, 054405 (2003).